Selective Extraction of REEs Thanks to One-Pot Silica Hybrid Materials

Robert Winkler, Stéphane Pellet-Rostaing, Guilhem Arrachart

applied sciences

MDPI

Article

Selective Extraction of REEs Thanks to One-Pot Silica Hybrid Materials

Robert Winkler *, Stéphane Pellet-Rostaing and Guilhem Arrachart *

ICSM, Univ Montpellier, CEA, CNRS, ENSCM, 30207 Marcoule, France; stephane.pellet-rostaing@cea.fr

* Correspondence: robert.winkler2292@web.de (R.W.); guilhem.arrachart@umontpellier.fr (G.A.); Tel.: +33-(46)-6791568 (G.A.)

Received: 8 September 2020; Accepted: 21 October 2020; Published: 27 October 2020

Abstract: The importance of rare-earth elements (REEs) in the global economy is rapidly growing, since they are essential to many advanced technologies. Therefore, the development of more performant separation procedures for REEs has become necessary. In the present study, we used silica hybrid materials (SHMs), which were synthesized by an all-in-one approach that allows the direct incorporation of desired functional groups, as sorbent material. Promising results were obtained for the extraction capacities of diglycolamide-functionalized materials. Under the tested conditions, they showed high efficiency (Nd uptake capacity of about 25 mg per g of material) and high selectivity toward REEs from a simulated NdFeB magnet leachate. For these materials, Nd recovery after extraction was achieved with an efficiency of 80% by contacting the loaded material with distilled water at moderate pH (6.5).

Keywords: silica hybrid material; rare earth elements; solid–liquid extraction; separation

1. Introduction

Rare-earth elements (REEs) play a crucial role in the functioning of current technology—e.g., electric motors, lighting, or information technology [1]. The mining process of REEs displays several challenges. The supply chain of REEs represents an economic and political issue due to the Chinese monopoly [2–4]. From an ecological point of view, REE mining bears the burden of large emissions, landscape and agricultural land destruction, and groundwater pollution [5,6]. With the surge of permanent magnet production, the REE demand was predicted to increase [1,2,7]. To meet the required quantities while limiting REE mining, a recycling-based circular economy would have many advantages [8]. First, if an application requires a combination of multiple REEs, the recycling process would recover these REEs close to or at the needed ratios. Second, REE recycling is performed in the regions that consume them, thus reducing cost and geopolitical difficulties. Third, compared to mining, REE recycling is less energy demanding, less polluting, and produces less CO_2 emissions [9].

Typical sources for REE recycling are manufacturing scraps, urban mining of end-of-life products, or industrial waste [8]. Considering the large in-use stocks of NdFeB permanent magnets, their recycling presents a good opportunity for urban mining [10].

However, the large shares of iron in typical leachates that hamper extraction require the use of highly selective and mechanically stable extraction materials [11]. Diglycolamic acid derivatives in various support materials were shown to fulfill these criteria [12–19]. Modified silica hybrid materials (SHMs) are an especially promising candidate for the recycling of REEs [20–22].

The materials in this work were prepared in an "all-in-one" approach to the sol-gel process, which uses customizable organosilane precursors. Previous studies [23–26] effectively showed the potential of this approach by linking the material structure to the self-assembly properties of the surfactant-like organosilane precursors, which can be conveniently described using the terminology of

surfactant science. Indeed, the precursors combine an organic function and a condensable group via a C11 alkyl chain that provides morphological similarity to classical surfactants (Figure 1). Organosilane precursors were synthesized by a Copper(I) catalyzed alkyne azide coupling (CuAAC) using a recyclable copper(I)-tren catalyst that allows the facile introduction of various functional groups [27]. The resulting materials were tested regarding REE extraction from NdFeB permanent magnets in consequential steps. First, the materials are screened for the adsorption of Neodymium. Then, the corresponding extraction mechanism(s) is (are) evaluated. Finally, the promising candidate(s) is (are) used for the extraction from a simulated leachate. For this study, the functional groups were selected to (i) evaluate the effect of the triazole group on extraction (SHM-1), (ii) check the extraction capacity of amine ligands (SHM-2), and (iii) compare the extraction properties of carboxylic acid and promising diglycolic acid derivatives (SHM-3, -4, and -5).

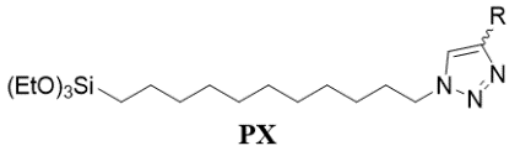

Figure 1. Typical structure of organosilane precursor PX used in this study for the synthesis of silica hybrid materials (SHMs) after a sol-gel process.

2. Materials and Methods

2.1. Material Synthesis and Characterizations

The organosilane sol-gel precursors were synthesized according to the procedure described in the literature through a CuAAC click reaction using a copper(I)-tren catalyst [26,27].

The procedure for preparing the silica hybrid materials starting from the organosilane sol-gel precursors was adapted from the procedure described in the literature [28,29]. Typically, 1.5 mmol of organosilane precursor PX were added to 50 mL of water. Afterwards, the pH was adjusted to basic (NH_4OH, pH 9) conditions for SHM-1 or acidic (HCl, pH 1.5) conditions for SHM-2 to SHM-5, and the solution was stirred for two weeks in a sealed flask. The basic conditions for SHM-1 were chosen because of the low yield under acidic conditions. SHM-3 was synthesized from the corresponding methyl ester organosilane precursor to give the intermediate material SHM-3-ME. The precipitate was dried by sublimation and washed with 60 mL (3 × 20 mL) EtOH/water (1/1) followed by 60 mL (3 × 20 mL) of EtOH. After analysis, the materials were heated to 130 °C for 24 h to promote the condensation.

The carboxylic acid functional group of SHM-3 was obtained in a second step from SHM-3-ME by an hydrolysis reaction inspired by the literature [30]. SHM-3-ME (1 eq) was stirred in an acetonitrile/water (94/6) solution containing LiBr (5 eq), NEt_3 (5 eq) for 3 days at 50 °C.

Finally, all SHMs were washed using 60 mL (3 × 20 mL) of each solution: first a NEt_3/EtOH/water (8/60/32) solution, followed by a EtOH/water (1/1) solution, then EtOH, then a EtOH/diethyl ether (1/1) solution, and finally with diethyl ether.

Solid-state FT-IR spectra were collected on a Perkin-Elmer 100 spectrometer (Perkin Elmer, Villebon S/Yvette, France) using an Attenuated Total Reflectance (ATR) crystal with a resolution of 4 cm^{-1}.

Thermogravimetric analysis (TGA) was performed using a Setaram Setsys Evolution 18 instrument (SETARAM Instrumentation, Caluire, France) under airflow (20 mL min^{-1}) with a heating rate of 5 °C min^{-1} coupled to a Hiden analytical QGA mass spectrometer (Hiden Analytical, Warrington, UK).

A Quanta 200 ESEM FEG scanning electron microscope (Thermo Fisher Scientific Electron Microscopy, Lyon France) was used for the morphological characterization of solids. Energy Dispersive X-ray Spectroscopy (X-EDS) analyses were performed thanks to the EDX XFlash® 5010 SDD analyzer (BRUKER SYNERGIE4, Evry, France) associated with the microscope.

Nitrogen adsorption–desorption isotherms were collected at 77 K using a Micromeritics ASAP 2020 apparatus (Micromeritics S.A., Verneuil en Halatte, France). Prior to the measurement, samples were desorbed at 60 °C for 12 h under vacuum.

2.2. Extraction Experiments

Experiments were carried out three times with an estimated uncertainty of 5%. For the present study, ultrapure water was used (Milli-Q®, 18 MΩ/cm). The metal-containing solutions were prepared by dilution of SCP Science ICP standard solutions. The desired pH was adjusted using nitric acid ([HNO_3] = 1×10^{-4}–0.1 M) taking into account the acidity of the standard solution (4% HNO_3). The simulated NdFeB permanent magnet leachate containing B (1.1 w%; 10 ppm), Co (1.6 w%; 15 ppm), Dy (1.3 w%; 12 ppm), Fe (67.2 w%; 630 ppm), Nd (24.5 w%; 230 ppm), Ni (0.6 w%; 6 ppm), and Pr (3.7 w%; 35 ppm) was prepared using SCP Science ICP standard solutions. The pH was adjusted to 1 using 1 M nitric acid taking into account the acidity of the stock solutions.

Extraction was performed by contacting the ground-up materials to the corresponding solution in the indicated ratios for 24 h under rotation (60 rpm). Afterwards, the solution was separated using centrifugation and filtration (0.2 µm cellulose acetate membrane) of the supernatant. Ion concentrations before and after extraction were determined using ICP-AES spectrometer (SPECTRO AMETEK, Kleve, Germany) or ICP-MS iCAP RQ spectrometer (Thermo Scientific, Les Ulis, France).

From the equations $Q_e = \left(C_i - C_f\right) * \frac{V}{m}$ and $E = \left(\frac{(C_i - C_f)}{C_i}\right) * 100$, the uptake capacity Q_e and the adsorption capacity E (%) were determined. In these equations, C_i and C_f refer to the ion concentration before and after contact and V/m refers to the solution volume to material mass ratio. The separation factor (SF) was calculated using the equation: $SF = \frac{M_1}{M_2} = \frac{QM_1}{QM_2}$. The isotherm for adsorption was investigated using the Langmuir $Q_e = Q_{max} \frac{L\, C_e}{1+L\, C_e}$ and Freundlich isotherms using $Q_e = K_F {C_e}^{1/n}$. In these equations, L refers to the Langmuir constant, Q_e to the quantity of adsorbed metal ions at equilibrium, Q_m to the adsorbent adsorption capacity, C_e to the equilibrium concentration of metal ions, and K_F to the Freundlich adsorption capacity constant.

2.3. Stripping

Back-extractions of REEs were studied by submitting the loaded hybrid material with pure water (MilliQ®) at room temperature. The material and the solution were separated by centrifugation over 10 min at 10,000 rpm in order to measure the metals' concentrations in the aqueous phase using ICP/AES. The stripping efficiency S (%) was calculated using the following equation: $S = ((Q_E - Q_F)/Q_E) * 100$, where Q_E refers to the metal ion concentration in SHM and Q_F to the residual metal ion concentration in the SHM.

3. Results and Discussion

3.1. Materials Characterization

Before beginning the extraction experiments, the obtained silsesquioxanes were characterized. First, the material composition was examined using FT-IR and TGA. All FT-IR spectra (Supplementary Materials Figure S1) show characteristic peaks at 3130 cm^{-1} assigned to the C-H stretching mode of the triazole moiety, at 2920 cm^{-1} and 2850 cm^{-1}, which are attributed to the CH_2 asymmetric and symmetric stretching modes, at 1460 cm^{-1}, which is assigned to the C = C stretching in the triazole moiety, at 1210 cm^{-1}, which is assigned to the Si-CH_2- stretching mode, and at 1020–930 cm^{-1}, which is attributed to the Si-OH stretching modes [31–33]. The presence of the triazole moiety and the conservation of the Si-C bond is therefore confirmed in all final materials. Additionally, the presence of the functional headgroup was confirmed from their characteristic peaks, such as a signal at 1660 cm^{-1} assigned to the N-H bending mode of the primary amine for SHM-2. The C = O stretching mode from the carboxylic acid was observed at ~1720 cm^{-1} for SHM-3, while strong transmittance bands

were observed at ~1650 cm^{-1}, corresponding to the amidic C = O stretching frequencies [34] of the diglycolamide for SHM-4 (the etheric C-O stretching at 1110 cm^{-1} was not detected due to the presence of the strong Si-O-Si signals). For SHM-5, the C = O stretching mode at ~1740 cm^{-1} was attributed to the ester, and ~1690 cm^{-1} was assigned to amide carbonyl stretching [35].

Hence, the material structure is validated in the form displayed in Figure 2. After heating to 130 °C for 24 h, the intensity of the peak between 1020 and 930 cm^{-1} significantly decreased in favor of an intensity increase of the Si-O-Si peaks. This indicates the progression of the material condensation.

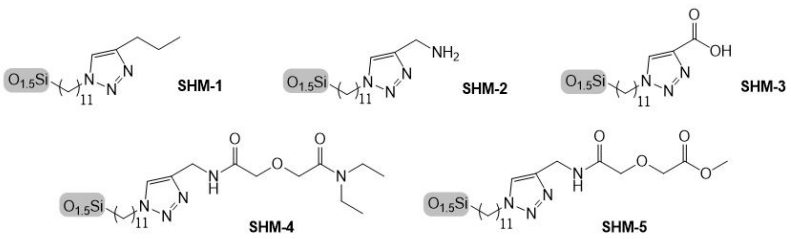

Figure 2. Silsesquioxanes investigated in this study.

Using TGA (Figure S2), the molecular weight of the silsesquioxane (M_{TGA}) was calculated by the equation $M_{TGA} = \frac{100}{w_{700\ °C}} * M_{SiO_2}$, where M_{SiO2} is the molecular weight of silica (60.09 g mol^{-1}) and $w_{700\ °C}$ is the constant residual weight percentage of the corresponding material. The results are shown in Table S1. The validity of this equation has been ensured by FT-IR results by verifying that the sample residue after TGA is pure silica.

The calculated molecular weights are in good agreement with the theoretical values for a fully condensed silsesquioxane. A rather complete condensation is inferred. This agrees with the observations from FT-IR. For the extraction experiments, the obtained molecular weights are used to determine the required material mass.

3.2. Extraction Properties

The extraction behavior of the screened SHMs (Figure 2) was first evaluated in batch extractions. Neodymium (Nd) extraction efficiencies were determined from the capacity or adsorption ability Q_e (mmol/g or mg/g) of the materials from solution assuming that equilibrium was reached after 24 h of contact at 25 °C. For each SHM, pH 1, 2, and 4 at a ligand (functional group) to metal ratio (L/M) of around 10 was used. The results are displayed in Figure 3.

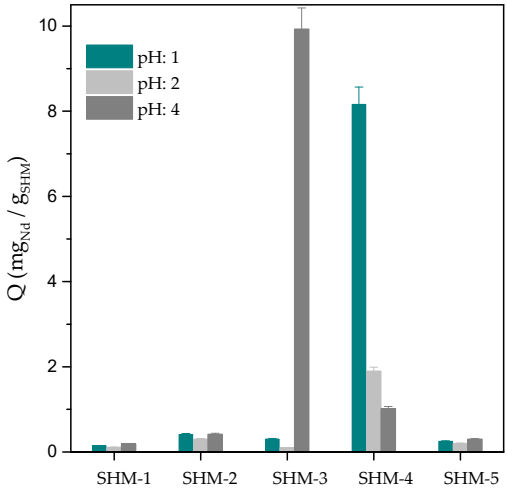

Figure 3. Nd extraction (Q_e) of the functionalized silica hybrid materials (SHMs). Initial conditions: pH = 1, 2, or 4, adjusted with HNO_3; [Nd] = 0.1 mmol/L (14.5 ppm)/volume 10 mL; functionalized materials, 5–7 mg: 0.015 mmol of functional group. Contact for 24 h at 25 °C.

The results show different extraction behaviors of the screened materials depending on their functional groups and the initial solution pH. Negligible amounts of adsorption are observed for the materials SHM-1, SHM-2, and SHM-5 regardless of pH. SHM-3 and SHM-4 show pH-dependent extraction behavior. Concerning this pH dependence, SHM-3 (carboxylic acid) only shows extraction at pH 4, while SHM-4 (diglycolamide) shows a decreasing extraction performance with increasing pH.

The low Q_e observed for SHM-1, SHM-2, and SHM-5 suggests that the triazole group alone is insufficient for the extraction of significant amounts of Nd under these conditions. To go further, in agreement with literature [36], it is valid to assume the non-participation of the triazole group. Therefore, the difference of extraction performance for all materials is assumed to be due to the different functional groups. This allows the discussion of the effects of the individual functional groups.

The amine group (SHM-2) does not extract Nd under the tested conditions, which is probably due to the protonation of the complex forming a free electron pair ($pK_A \approx 10.6$). Considering that the carboxylic acid (SHM-3) shows extraction only at pH 4, the driving force seems to be the ion exchange between the proton and the Nd-ion. This extraction mechanism is known for carboxylic acids, but is unspecific towards REEs [37]. The situation is more complicated for the diglycolic acid derivatives (SHM-4 and SHM-5).

The replacement of the diethyl amide by a methyl ester leads to a loss of the extraction performance towards Nd. In agreement with Ogata et al. [14], this is explicable by the electron donor capacity of the oxygen atoms in the diglycolic structure. Indeed, for SHM-4 and SHM-5, the first (secondary amide) and second (ether) oxygen participate in the complexation and are identical in SHM-4 and SHM-5. The third oxygen (amide in SHM-4, ester in SHM-5) has a different propensity to contribute its free electrons for metal complexation depending on the functionality. Generally, amides show better complexation than esters. In the present case, it is not only better, but exclusive. The tendency towards better performance at lower pH is a general feature of non-ionic extraction mechanisms like observed for neutral ligands, such as with diglycolamides in liquid–liquid extraction. There, increasing the feed nitric acid concentration causes an increase in the distribution ratio [38,39].

Considering the results, it is possible to desorb Nd by adjusting the pH of the solution. To this end, the recovered solid phase after extraction at pH 1 of SHM-4 loaded with Nd was contacted with pure water (Milli-Q) at pH 6.5 at a volume to solid ratio similar to that for the extraction (V = 10 mL, m(SHM-4) = 7 mg). As expected from the decreasing extraction performance at increasing pH, a large quantity of Nd was stripped (80%). The corresponding data are shown in Table 1.

Table 1. Recovery of Nd from the loaded extraction of solid phase SHM-4. Extraction condition: [Nd] = 0.1 mmol/L (14.5 ppm) pH = 1 + SHM-4 (7 mg: 0.015 mmol of functional group). Contact for 24 h at 25 °C. Stripping condition: Nd-loaded SHM-4: 7 mg + Milli-Q water pH: 6.5 (volume 10 mL). Contact for 24 h at 25 °C.

	[C] (g/L)	V (mL)	C_i (ppm)	C_f (ppm)	%Efficiency
Extraction	0.7	13.50	14.53	8.49	42%
Stripping			6.04	4.98	82%

3.3. Mechanism of the Nd Extraction by SHM-4

The isotherm for adsorption of the Nd onto SHM-4 at 25 °C was prepared from nitric acid solutions (pH 1) at different Nd concentrations (1–250 mg/L). Other parameters were kept constant (V/m = 10). The Langmuir isotherm results are illustrated in Figure 4.

Figure 4 shows the uptake capacity (black) and the modified uptake capacity (red). The uptake capacity shows a saturation at Nd concentrations above 0.007 mmol/L. Fitting the modified uptake capacity (red) with the Langmuir equation $Q_e = Q_{max} \frac{L\ C_e}{1+L\ C_e}$ leads to a solid R^2 value (0.9962).

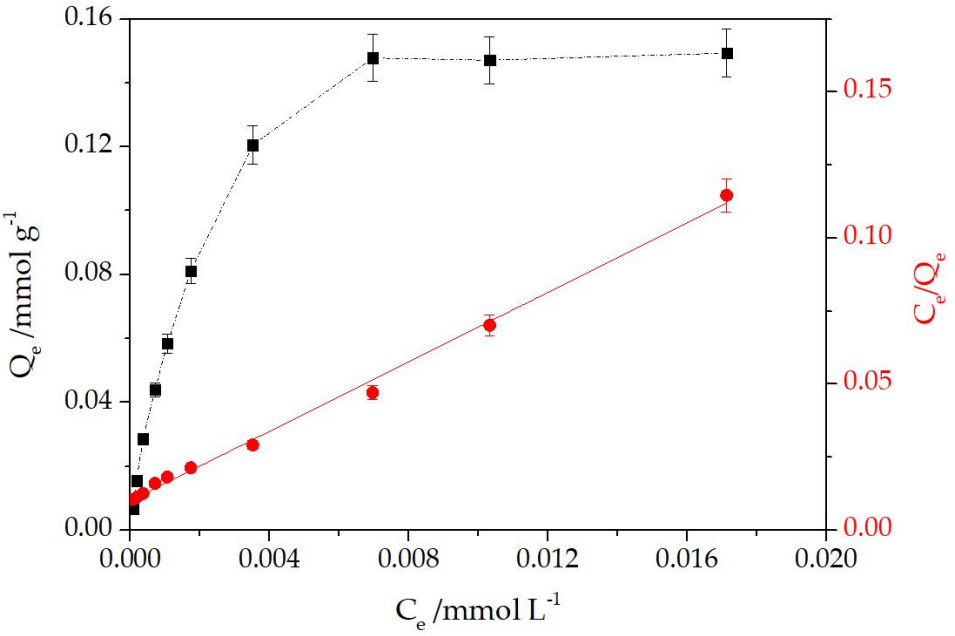

Figure 4. Isotherm for adsorption of neodymium on SHM-4 at 25 °C and linear regression of the Langmuir model (*Ce*/*Qe* = f(*Ce*): y = 5.95(±0.13)x + 0.1001(±0.0009); R^2 = 0.996. Initial pH 1.0 adjusted with HNO_3; [Nd] = 1–250 ppm/volume, 10 mL SHM-4: 5 mg.

This result indicates the formation of a monolayer where all Nd adsorption sites are equal in energy. From this, it can be concluded that all sites where Nd is adsorbed are similar in energy and a monolayer is formed. For comparison, the Freundlich isotherm $Q_e = K_F C_e^{1/n}$ was also investigated (Figure S3). It would suggest the energetic heterogeneity of the adsorption sites. Plotting Ln(Q_e) = f(Ln(C_e), an unsatisfactory R^2 value of 0.94 is obtained, excluding this behavior.

From this, a maximum extraction capacity Q_{max} for Nd was determined to be 0.168 mmol/g (24.25 mg/g). Compared to the literature, this value is superior to the values found by Juère et al. [16], who investigated diglycolamide-functionalized mesoporous silica (200 µg/g), and is similar to the studies of Ogata et al., who investigated diglycol amic acid functional groups (Q_{max} = 16 mg/g) [13].

Small amounts of adsorbed nitrogen were measured for the materials from N_2 adsorption/desorption measurements. However, this is typical of the investigated materials and irrelevant for the accessibility of functional groups, as shown by the extraction results and in the literature [40]. To investigate the presence of Nd in SHM more closely, SEM-EDX analyses were performed. Figure 5 shows the resulting images.

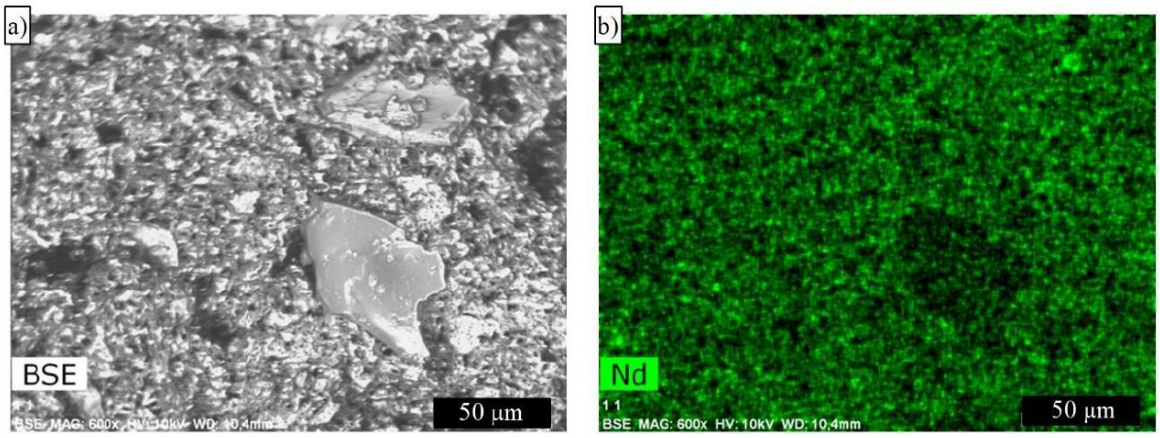

Figure 5. SEM-EDX mapping of SHM-4 after contacting solution with Nd: (**a**) SHM-4 morphology; (**b**) spatial distribution of Nd.

At the observed scale, an even distribution of Nd in SHM-4 can be assumed after the extraction (Figure 5b). This indicates that, after 24 h of contact, the material was effectively filled with the solution and that the equilibrium was reached. Moreover, from the EDX measurements, the elemental composition of materials (Figure S4) was determined. A molar ratio of Nd/Si = 0.103 was estimated, which is close to the ratio determined from Q_{max} (Nd/Si = 0.080 ± 0.005) assuming a molecular weight of SHM-4 of about 481 ± 30 g mol^{-1}.

3.4. Extraction of Rare-Earth Elements (Nd, Pr, Dy) towards Competitive Elements

The obtained results suggest the application of SHM-4 for the recycling of NdFeB permanent magnets, while SHM-3 was not investigated due to its unspecificity toward REEs, as mentioned earlier. To investigate this, extraction experiments were performed using a simulated leachate, HNO_3 at pH 1, which contained Nd next to other typical REEs like Pr and Dy as well as typical competitive ions like B, Co, Ni, and Fe. The exact composition of the solution is given in Table 2.

Table 2. Composition of the simulated leachate of a NdFeB magnet.

Elements	B	Co	Dy	Fe	Nd	Ni	Pr
w%	1.1	1.6	1.3	67.2	24.5	0.6	3.7
Concentration (ppm)	11.32	15.45	12.35	641.6	218.7	3.05	34.34

In this experiment, the solution/solid ratio was between 125 and 3500 (V = 1–25 mL; m = 7.5 mg), which corresponds to a material concentration between 8 and 0.3 g/L. The results are illustrated in Figure 6.

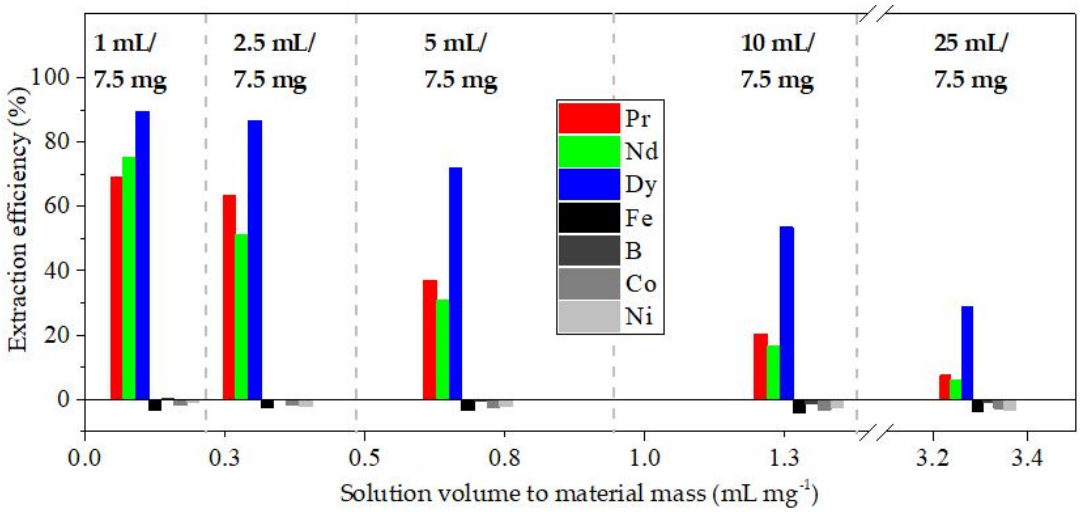

Figure 6. Extraction efficiencies (Q_e) of the different metals present in the described permanent magnet leachate as a function of the quantity of functionalized SHM-4. Initial conditions: pH = 1; composition, see Table 2; volume $_{(Solution)}$ = 1–25 mL; m $_{(SHM-4)}$ = 7.5 mg. Contact for 24 h, T = 25 °C.

Whatever the concentration, only REEs were extracted; this result in is good agreement with the specificity of the diglycolamide functional group for lanthanides [41,42]. Negative values for the non-REEs indicate that the extraction quantities are below the detection limit. Even with a large excess of ligands (V/m = 1 mL/7.5 mg), no extraction of competitive ions was observed. At increasing solution volume, the percentage of extracted ions decreases because the metal uptake capacity of the material reaches saturation (Figure S5). The specificity for the REEs was also highlighted when the experiments were performed at constant metal concentration and by increasing the concentration of the material engaged in the extraction (Table S2).

The obtained results show the potential of SHM-4 for the highly selective extraction of NdFeB magnet leachates that contain large quantities of Fe (>65 w%). Even under these conditions, separation factors $SF_{(REE/Fe)} > 100$ were obtained even when the concentration of the material was about 7.5 g/L.

4. Conclusions

Silica hybrid materials (SHMs) were engaged in extraction experiments in relation to NdFeB permanent magnets. Mechanistically, it was found that the Nd extraction by SHMs occurs without the involvement of the triazole linker, validating the use of this linker to obtain functional SHMs for the selective extraction of metals of interest, such as REEs. Furthermore, the functionalization with the diglycolamide group (SHM-4) was identified as a promising candidate for the efficient and highly selective extraction of REEs from NdFeB simulated leachates.

Indeed, the first experiments on a pure Nd solution indicate that the equilibrium is reached in <24 h and that the recovery of the extracted REEs from the loaded material can be achieved using Milli-Q water. To evaluate the reusability of the investigated materials, consecutive extraction and stripping steps should be investigated. Diffusion into the materials appears not to be a hindering factor. In a second experiment, using a simulated NdFeB leachate in nitric acid (pH 1), none of the typical competitive ions were extracted, while the REEs were selectively extracted.

Supplementary Materials: The following are available online at http://www.mdpi.com/2076-3417/10/21/7558/s1: Figure S1. FT-IR spectra of the synthesized materials before and after the thermal treatment. Figure S2. TGA of the synthesized materials after the thermal treatment. Table S1. Residual weight after TGA and the corresponding molecular weights of the synthesized SHMs. Figure S3. Linear regression of the Freundlich model. Figure S4. EDX spectrum and elemental composition for the Nd loaded SHM-4. Table S2. Details of extraction efficiencies and Q values from the multi-element solution. Figure S5. Quantities of metals as a function of the solution volume to material mass ratio (V/m).

Author Contributions: Conceptualization, R.W., S.P.-R., and G.A.; methodology, R.W., S.P.-R., and G.A.; validation, S.P.-R. and G.A.; formal analysis, R.W.; investigation, R.W.; writing—original draft preparation, R.W. and G.A.; writing—review and editing, R.W. and G.A.; supervision, S.P.-R. and G.A.; project administration, S.P.-R. and G.A. All authors have read and agreed to the published version of the manuscript.

Funding: This research received no external funding.

Acknowledgments: The authors acknowledge C. Rey and B. Baus Lagarde for their technical support.

Conflicts of Interest: The authors declare no conflict of interest.

References

1. Balaram, V. Rare earth elements: A review of applications, occurrence, exploration, analysis, recycling, and environmental impact. *Geosci. Front.* **2019**, *10*, 1285–1303. [CrossRef]
2. Goodenough, K.M.; Wall, F.; Merriman, D. The rare earth elements: Demand, global resources, and challenges for resourcing future generations. *Nat. Resour. Res.* **2018**, *27*, 201–216. [CrossRef]
3. European Commission. *Critical Raw Materials Resilience: Charting a Path towards Greater Security and Sustainability*; COM(2020) 474 Final; European Commission: Brussel, Belgium, 2020.
4. U.S. Department of Energy. *Critical Materials Strategy*; U.S. Department of Energy: Washington, DC, USA, 2011.
5. Kumari, A.; Panda, R.; Jha, M.K.; Kumar, J.R.; Lee, J.Y. Process development to recover rare earth metals from monazite mineral: A review. *Min. Eng.* **2015**, *79*, 102–115. [CrossRef]
6. Sengupta, M. *Environmental Impacts of Mining: Monitoring, Restoration, and Control*; Routledge: New York, NY, USA, 2018.
7. Li, X.Y.; Ge, J.P.; Chen, W.Q.; Wang, P. Scenarios of rare earth elements demand driven by automotive electrification in China: 2018–2030. *Resour. Conserv. Recycl.* **2019**, *145*, 322–331. [CrossRef]
8. Yoon, H.S.; Kim, C.J.; Chung, K.W.; Kim, S.D.; Lee, J.Y.; Kumar, J.R. Solvent extraction, separation and recovery of dysprosium (Dy) and neodymium (Nd) from aqueous solutions: Waste recycling strategies for permanent magnet processing. *Hydrometallurgy* **2016**, *165*, 27–43. [CrossRef]

9. Yang, Y.; Walton, A.; Sheridan, R.; Güth, K.; Gauß, R.; Gutfleisch, O.; Buchert, M.; Steenari, B.M.; Van Gerven, T.; Jones, P.T.; et al. REE recovery from end-of-life NdFeB permanent magnet scrap: A critical review. *J. Sustain. Metall.* **2017**, *3*, 122–149. [CrossRef]
10. Du, X.; Graedel, T.E. Global rare earth in-use stocks in NdFeB permanent magnets. *J. Ind. Ecol.* **2011**, *15*, 836–843. [CrossRef]
11. Lixandru, A.; Poenaru, I.; Güth, K.; Gauß, R.; Gutfleisch, O. A systematic study of HDDR processing conditions for the recycling of end-of-life Nd-Fe-B magnets. *J. Alloys Compd.* **2017**, *724*, 51–61. [CrossRef]
12. Ogata, T.; Narita, H.; Tanaka, M. Immobilization of diglycol amic acid on silica gel for selective recovery of rare earth elements. *Chem. Lett.* **2014**, *43*, 1414–1416. [CrossRef]
13. Ogata, T.; Narita, H.; Tanaka, M. Adsorption behavior of rare earth elements on silica gel modified with diglycol amic acid. *Hydrometallurgy* **2015**, *152*, 178–182. [CrossRef]
14. Ogata, T.; Narita, H.; Tanaka, M. Adsorption mechanism of rare earth elements by adsorbents with diglycolamic acid ligands. *Hydrometallurgy* **2016**, *163*, 156–160. [CrossRef]
15. Florek, J.; Chalifour, F.; Bilodeau, F.; Larivière, D.; Kleitz, F. Nanostructured hybrid materials for the selective recovery and enrichment of rare earth elements. *Adv. Funct. Mater.* **2014**, *24*, 2668–2676. [CrossRef]
16. Juère, E.; Florek, J.; Larivière, D.; Kim, K.; Kleitz, F. Support effects in rare earth element separation using diglycolamide-functionalized mesoporous silica. *New J. Chem.* **2016**, *40*, 4325–4334. [CrossRef]
17. Besnard, R.; Winkler, R.; Arrachart, G.; Cambedouzou, J.; Pellet-Rostaing, S. Ion extraction applications of bilayer-structured hybrid silicas. *Mater. Chem. Front.* **2018**, *2*, 1031–1039. [CrossRef]
18. Shinozaki, T.; Ogata, T.; Kakinuma, R.; Narita, H.; Tokoro, C.; Tanaka, M. Preparation of polymeric adsorbents bearing diglycolamic acid ligands for rare earth elements. *Ind. Eng. Chem. Res.* **2018**, *57*, 11424–11430. [CrossRef]
19. Arrambide, C.; Arrachart, G.; Berthalon, S.; Wehbie, M.; Pellet-Rostaing, S. Extraction and recovery of rare earths by chelating phenolic copolymers bearing diglycolamic acid or diglycolamide moieties. *React. Funct. Polym.* **2019**, *142*, 147–158. [CrossRef]
20. Arrachart, G.; Karatchevtseva, I.; Cassidy, D.J.; Triani, G.; Bartlett, J.R.; Wong Chi Man, M. Synthesis and characterisation of carboxylate-terminated silica nanohybrid powders and thin films. *J. Mater. Chem.* **2008**, *18*, 3643–3649. [CrossRef]
21. Zheng, X.D.; Wang, C.; Dai, J.D.; Shi, W.D.; Yan, Y.S. Design of mesoporous silica hybrid materials as sorbents for the selective recovery of rare earth metals. *J. Mater. Chem. A* **2015**, *3*, 10327–10335. [CrossRef]
22. Hu, Y.M.; Florek, J.; Lariviere, D.; Fontaine, F.G.; Kleitz, F. Recent advances in the separation of rare earth elements using mesoporous hybrid materials. *Chem. Rec.* **2018**, *18*, 1261–1276. [CrossRef]
23. Alauzun, J.; Mehdi, A.; Mouawia, R.; Reyé, C.; R.Corriu, J.P. Synthesis of new lamellar materials by self-assembly and coordination chemistry in the solids. *J. Sol. Gel Sci. Technol.* **2008**, *46*, 383–392. [CrossRef]
24. Besnard, R.; Arrachart, G.; Cambedouzou, J.; Pellet-Rostaing, S. Tuning the nanostructure of highly functionalized silica using amphiphilic organosilanes: Curvature agent effects. *Langmuir* **2016**, *32*, 4624–4634. [CrossRef]
25. Besnard, R.; Arrachart, G.; Cambedouzou, J.; Pellet-Rostaing, S. Tuning the morphology of functionalized silica using amphiphilic organosilanes. *J. Sol. Gel Sci. Technol.* **2017**, *81*, 452–467. [CrossRef]
26. Winkler, R. Development of an "all in one" approach for the synthesis of silica-based hybrid materials. Ph.D. Thesis, ICSM. University Montpellier, Montpellier, France, 2019.
27. Winkler, R.; Pellet-Rostaing, S.; Arrachart, G. Improvement of organosilane synthesis through click chemistry. *Tetrahedron Lett.* **2020**. [CrossRef]
28. Besnard, R.; Cambedouzou, J.; Arrachart, G.; Diat, O.; Pellet-Rostaing, S. Self-assembly of condensable "bola-amphiphiles" in water/tetraethoxysilane mixtures for the elaboration of mesostructured hybrid materials. *Langmuir* **2013**, *29*, 10368–10375. [CrossRef] [PubMed]
29. Besnard, R.; Arrachart, G.; Cambedouzou, J.; Pellet-Rostaing, S. Structural study of hybrid silica bilayers from "bola-amphiphile" organosilane precursors: Catalytic and thermal effects. *RSC Adv.* **2015**, *5*, 57521–57531. [CrossRef]
30. Mattsson, S.; Dahlström, M.; Karlsson, S. A mild hydrolysis of esters mediated by lithium salts. *Tetrahedron Lett.* **2007**, *48*, 2497–2499. [CrossRef]
31. Al-Oweini, R.; El-Rassy, H. Synthesis and characterization by FTIR spectroscopy of silica aerogels prepared using several $Si(OR)_4$ and $R''Si(OR')_3$ precursors. *J. Mol. Struct.* **2009**, *919*, 140–145. [CrossRef]

32. Creff, G.; Arrachart, G.; Hermet, P.; Wadepohl, H.; Almairac, R.; Maurin, D.; Sauvajol, J.L.; Carcel, C.; Moreau, J.J.E.; Dieudonné, P.; et al. Investigation on the vibrational and structural properties of a self-structured bridged silsesquioxane. *Phys. Chem. Chem. Phys.* **2012**, *14*, 5672–5679. [CrossRef]
33. Arkles, B.; Larson, G. *Silicon Compounds: Silanes & Silicones*; Gelest: Morrisville, PA, USA, 2013.
34. Rama Swami, K.; Kumaresan, R.; Nayak, P.K.; Venkatesan, K.A.; Antony, M.P. Extraction of Eu(III) in diglycolamide-organophosphorous acid and the interaction of binary solution with Eu(III) studied by FTIR spectroscopy. *Vib. Spectrosc.* **2017**, *93*, 1–11. [CrossRef]
35. Kubelka, J.; Keiderling, T.A. Ab Initio calculation of amide carbonyl stretch vibrational frequencies in solution with modified basis Sets. 1. *N*-Methyl Acetamide. *J. Phys. Chem. A* **2001**, *105*, 10922–10928. [CrossRef]
36. Wehbie, M.; Arrachart, G.; Arrambide Cruz, C.; Karamé, I.; Ghannam, L.; Pellet-Rostaing, S. Organization of diglycolamides on resorcinarene cavitand and its effect on the selective extraction and separation of HREEs. *Sep. Purif. Technol.* **2017**, *187*, 311–318. [CrossRef]
37. Preston, J.S. Solvent extraction of metals by carboxylic acids. *Hydrometallurgy* **1985**, *14*, 171–188. [CrossRef]
38. Moktli, B.; Poitrenaud, C. Medium effect on the separation factor in liquid-liquid extraction. Application to the separation of trtvalent lanthanide nitrates by tri-n-butylphosphate. *Solvent Extr. Ion. Exch.* **1997**, *15*, 455–481. [CrossRef]
39. Wehbie, M.; Arrachart, G.; Karamé, I.; Ghannam, L.; Pellet-Rostaing, S. Triazole Diglycolamide Cavitand for lanthanide extraction. *Sep. Purif. Technol.* **2016**, *169*, 17–24. [CrossRef]
40. Besnard, R.; Cambedouzou, J.; Arrachart, G.; Le Goff, X.F.; Pellet-Rostaing, S. Organosilica-metallic sandwich materials as precursors for palladium and platinum nanoparticle synthesis. *RSC Adv.* **2015**, *5*, 77619–77628. [CrossRef]
41. Ansari, S.A.; Mohapatra, P.K. A review on solid phase extraction of actinides and lanthanides with amide based extractants. *J. Chromatogr. A* **2017**, *1499*, 1–20. [CrossRef]
42. Ansari, S.A.; Pathak, P.; Mohapatra, P.K.; Manchanda, V.K. Chemistry of diglycolamides: Promising extractants for actinide partitioning. *Chem. Rev.* **2012**, *112*, 1751–1772. [CrossRef]